Generalized Multi-gridding Technique for the TLM Method using the Symmetrical Super-Condensed Node (SSCN)

G.N.Mulay and Mrs. K.S.Jog

G. N. Mulay is with the Dept. of Electronics & Telecommunications, Maharashtra Institute of Technology, Pune 411038, India and Mrs K.S.Jog is with the Government College of Engineering, Pune 411005, India

***Abstract* — This paper extends Wlodarcyzk's TLM multi-gridding-technique to the generalized one & two dimensional cases wherein the fine meshes can have different lengths & widths. The advantage is that it is no longer necessary to divide the problem space into separate 'coarse' & 'fine' regions which provides for considerable meshing flexibility. Equations describing the connection procedure for the SSCN are derived. Modelling of cross-talk between PCB tracks is implemented with this new method and the simulation results compared with experiments.**

I. Introduction

In common with other techniques, graded meshing or multi-gridding is generally required when using the transmission line matrix (TLM) method [1] for the analysis of electromagnetic field problems. With multi-gridding, a mesh can have more than one neighbour in each direction, and for this, a recently introduced node formulation, the symmetrical super-condensed node (SSCN) [2] provides considerable flexibility as non-uniform mesh structures can be modelled without using stubs and with a greater time-step.

Of the two methods previously proposed for multi-gridding, the first, by Herring [3], uses space & time approximations to pass voltage pulses across the interface between the coarse & fine regions while the second, by Wlodarcyzk [4], uses ideal transformers to electrically connect the coarse & fine region meshes, with the fine meshes having nominally the same size & shape.

In this paper, this second method is modified to cover the general one & two-dimensional cases where the fine meshes are flush-aligned with each other but do not have the same size or shape.

II. One-dimensional multi-gridding

The general case is shown in Fig. 1, for multi-gridding in the +X direction and represents a *m* x 1 (fine) to 1 (coarse) interface, with all mesh dimensions being in multiples of *lo*, the equivalent cubic cell parameter of the background region [2]. The connection procedure for obtaining the reflected pulses from the pulses incident on the interface is described for both polarizations.

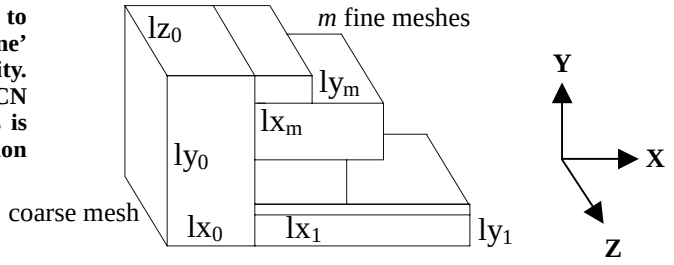

Fig. 1. One dimensional multi-gridding interface.

A..Y Polarization

Applying the concepts in [4] to the interface, the meshes are replaced by ideal transformers with turns ratios equal to the aspect ratios of the mesh faces. Hence for the coarse mesh ($i = j = 0$) and the jth fine mesh ($i = 1$, $j = 1,2\ldots m$), these turns ratios are (all meshes have the same *lz0)*

$$f_{00} = \frac{\Delta z_0}{\Delta y_0} = \frac{lz_0 l_0}{ly_0 l_0} = \frac{lz_0}{ly_0},\ f_{1j} = \frac{\Delta z_0}{\Delta yj} = \frac{lz_0}{lyj} \qquad (1)$$

Since there is only a single column of fine meshes along the direction of polarization, the secondaries of the corresponding transformers are all connected in parallel and finally connected in parallel with the secondary of the coarse mesh transformer. With this, the Thevenin equivalent incident pulse voltages, V_j, the link-line characteristic admittances, Y_j, and the winding currents I_j, all referred to the secondaries are, respectively

$$V_0 = 2 f_{00} V^{rf}_{xpy0}, \qquad Vj = 2 f_{1j} V^{rf}_{xny\,j} \qquad (2)$$

$$Y_0 = \frac{1}{f_{00}{}^2 Z_{xy0}}, \qquad Y_j = \frac{1}{f_{1j}{}^2 Z_{xy\,j}} \qquad (3)$$

$$\mathrm{I}_0 = V_0 Y_0 = \frac{2V^{rf}_{xpy0}}{f_{00} Z_{xy0}}, \quad \mathrm{Ij} = VjYj = \frac{2V^{rf}_{xny\,j}}{f_{1j} Z_{xy\,j}} \qquad (4)$$

where V^{rf}_{xpy0} is the +X directed Y polarized incident pulse coming from the coarse mesh and $V^{rf}_{xny\ j}$ is the –X

directed Y polarized incident pulse coming from the *j*th fine mesh.

The total incident secondary-side nodal voltage is

$$V_{xy} = \frac{I_0 + \sum_{j=1}^{m} I_j}{Y_0 + \sum_{j=1}^{m} Y_j} = b_0 V^{rf}_{xpy0} + \sum_{j=1}^{m} bj V^{rf}_{xny\,j} \qquad (5)$$

To obtain coefficients $b_0 \ldots b_m$, the link-line characteristic impedances *Zxyj* in (4) have to be expressed in terms of the mesh parameters [2] viz.

$$Z_{xy} = \frac{\Delta y}{\Delta x \Delta z}\frac{l_0}{2C^{\wedge}_{xy}}\sqrt{\frac{\mu}{\varepsilon}} = \frac{ly_0}{2C^{\wedge}_{xy} lx_0 lz_0 \sqrt{\varepsilon_r \mu_r}}\sqrt{\frac{\mu}{\varepsilon}}$$

$$= \frac{ly_0 Z_0}{2C^{\wedge}_{xy} lx_0 lz_0 \varepsilon_r} \qquad (6)$$

where $C^{\wedge}_{xy}$ = normalized *xy* link-line capacitance
Z_0 = impedance of background region
ε_r = relative permittivity

Substituting (6) in (5) and using (1) to (4), we get, after some simplification, for the coarse and fine meshes

$$b_0 = lx_0 \varepsilon_{r0} C^{\wedge}_{xy0} E_{xy}, \qquad bj = lxj \varepsilon_{rj} C^{\wedge}_{xy\,j} E_{xy} \qquad (7)$$

$$\text{with} \quad E_{xy} = \frac{2lz_0}{ly_0 lx_0 \varepsilon_{r0} C^{\wedge}_{xy0} + \sum_{j=1}^{m} lyj lxj \varepsilon_{rj} C^{\wedge}_{xy\,j}} \qquad (8)$$

Finally, the reflected pulses from the interface are given by [4]

$$V^{in}_{xpy\,0} = V^{rf}_{xpy\,0} + (V_{xy} - V_0) Y_0 f_{00} Z_{xy0}$$

$$V^{in}_{xny\,j} = V^{rf}_{xny\,j} + (V_{xy} - V_{1j}) Y_{1j} f_{1j} Z_{xyj}$$

where V^{in}_{xpy0} & V^{in}_{xnyj} are the reflected pulses in the coarse mesh and *j*th fine mesh. Using (1) to (4), the final simplified expressions for the reflected pulses are

$$V^{in}_{xpy0} = \frac{V_{xy}}{f_{00}} - V^{rf}_{xpy0} \qquad (9)$$

$$V^{in}_{xnyj} = \frac{V_{xy}}{f_{1j}} - V^{rf}_{xnyj} \qquad (10)$$

B.Z Polarization

As the aspect ratios of the meshes for this polarization will be the reciprocals of the corresponding ratios for the Y polarization, the transformer turns ratios will also be reciprocals viz. for the coarse mesh ($i = j = 0$) and the *i*th fine mesh ($i = 1,2\ldots m$, $j = 1$), these turns ratios are

$$f_{00} = \frac{ly_0}{lz_0}, \qquad f_{i1} = \frac{ly_i}{lz_0} \qquad (11)$$

Here, along the direction of polarization , there are *m* columns of fine meshes each having a single row. Therefore, the secondaries of all these transformers are series co-nnected and then connected in parallel with the secondary of the coarse mesh transformer.With this, the Thevenin equivalent incident pulse voltages and the link-line characteristic admittances referred to the secondary are

$$V_0 = 2 f_{00} V^{rf}_{xpz0}, \qquad V_1 = 2\sum_{i=1}^{m} f_{i1} V^{rf}_{xnzi} \qquad (12)$$

$$Y_0 = \frac{1}{f_{00}^{\,2} Z_{xz0}}, \qquad Y_1 = \frac{1}{\sum_{i=1}^{m} f_{i1}^{\,2} Z_{xzi}} \qquad (13)$$

The total incident secondary-side nodal voltage is now directly obtained as

$$V_{xz} = \frac{V_0 Y_0 + V_1 Y_1}{Y_0 + Y_1} \qquad (14)$$

while the reflected pulses are given by

$$V^{in}_{xpz0} = V^{rf}_{xpz0} + (V_{xz} - V_0) Y_0 f_{00} Z_{xz0}$$

$$V^{in}_{xnzi} = V^{rf}_{xnzi} + (V_{xz} - V_1) Y_1 f_{i1} Z_{xzi}$$

Using (11) to (14) the above can be finally re-written as

$$V^{in}_{xpz0} = V^{rf}_{xpz0} + c_0 F_{xz}, \quad V^{in}_{xnzi} = V^{rf}_{xnzi} + ci F_{xz} \qquad (15)$$

where

$$F_{xz} = -f_{00} V^{rf}_{xpz0} + \sum_{i=1}^{m} f_{i1} V^{rf}_{xnzi} \qquad (16)$$

$$c_0 = \frac{2Y_1}{f_{00}(Y_0 + Y_1)} = \frac{2lz_0}{ly_0}\frac{1}{1 + \frac{lx_0}{ly_0}\varepsilon_{r0} C^{\wedge}_{xz0} \sum_{i=1}^{m} \frac{lyi}{lxi \varepsilon_{ri} C^{\wedge}_{xzi}}} \qquad (17)$$

$$ci = -\frac{2Y_1 Y_0}{(Y_0 + Y_1)} f_{i1} Z_{xzi} = -c_0 \frac{lx_0 \varepsilon_{r0} C^{\wedge}_{xz0}}{lxi \varepsilon_{ri} C^{\wedge}_{xzi}} \qquad (18)$$

where $C^{\wedge}_{xz}$ is the normalized xz link-line capacitance and

V^{in}_{xpy0} & V^{in}_{xnyi} are the reflected pulses in the coarse mesh and ith fine mesh, respectively.

III. TWO-DIMENSIONAL MULTI-GRIDDING

The general case shown in Fig. 2, for 2D multi-gridding in the +Z direction represents a *m* to 1 interface, in which *m* fine meshes, having different lengths & breadths, but which are flush-aligned with each other, connect with a single coarse mesh of size lx_0 x ly_0 (in multiples of *lo).*

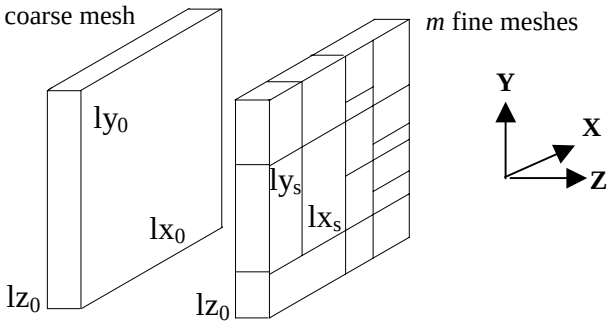

Fig. 2. Two dimensional multi-gridding interface

The *m* fine meshes are first replaced by a total of lx_0 x ly_0 meshes, each of size 1 x 1, as follows:

A .X Polarization

Replace the *s*th mesh of size *lxs* x *lys* having an incident pulse of V^{rf}_{znxs} and link-line impedance Z_s, located at (*xs ys)* w.r.t. the origin of the coarse mesh, by *lxs* x *lys* meshes, each of size 1 x 1, having incident pulses and link-line impedances given by

$$U_{xs+i,\,ys+j} = \frac{V^{rf}_{znxs}}{lys}\,,\; Z_{xs+i,\,ys+j} = Z_s \frac{lxs}{lys} \qquad (19)$$

with $i = 1,2,\ldots lxs,\;\; j = 1,2,\ldots lys,$ and $s = 1,2,\ldots m$

The above are obtained by noting that, as per [4], for the horizontal (X) polarization, all *lys* mesh secondaries in a column are connected in series and then each of these *lxs* columns are connected in parallel.

Applying the equations in [4] directly to this new lx_0 x ly_0 by 1 interface, the transformer turns ratios for the coarse mesh (i = j = 0) and the (i,j)th fine mesh (i = 1,2…lx_0, j = 1,2…ly_0) are

$$f_{00} = \frac{\Delta y_0}{\Delta x_0} = \frac{ly_0}{lx_0}\,, \quad f_{ij} = \frac{\Delta y_{ij}}{\Delta x_{ij}} = 1 \qquad (20)$$

Noting that, unlike in [4], all series connected *lij* meshes in the *i*th column will not, in general, have the same link-line impedance, the Thevenin equivalent incident pulse voltages, V_i, and the link-line characteristic admittances, Y_i, for that column, referred to the secondaries, are

$$V_0 = 2 f_{00} V^{rf}_{zpx0}\,, \qquad Vi = 2\sum_{j=1}^{ly0} f_{ij} U_{ij} \qquad (21)$$

$$Y_0 = \frac{1}{f_{00}^{\,2} Z_{00}}\,, \quad Yi = \frac{1}{\sum_{j=1}^{ly0} f_{ij}^{\,2} Z_{ij}} = \frac{1}{\sum_{j=1}^{ly0} Z_{ij}} \qquad (22)$$

The total incident secondary-side nodal voltage is

$$V_{xy} = \frac{V_0 Y_0 + \sum_{i=1}^{lx0} ViYi}{Y_0 + \sum_{i=1}^{lx0} Yi} \qquad (23)$$

and the reflected voltages are then given by

$$V_{ij} = U_{ij} + (V_{xy} - V_i) Y_i f_{ij} Z_{ij}$$

For the coarse mesh, using (19) to (23), we get

$$V^{in}_{zpx0} = \frac{V_{xy}}{f_{00}} - V^{rf}_{zpx0} \qquad (24)$$

For the lx_0 x ly_0 fine meshes, *fij* =1.Hence the final step of reconverting the *lxs* x *lys* reflected pulses of the meshes located in the area corresponding to the original *s*th mesh, into a single pulse is done by averaging the reflected voltages of the *lxs* x *lys* meshes and then multiplying by the number of column meshes, *lys*; thus

$$V^{in}_{znxs} = \frac{1}{lxs}\sum_{i=1}^{lxs}\sum_{j=1}^{lys} V_{xs+i,\,ys+j} \qquad (25)$$

B .Y Polarization

The analysis and formulae for this case are identical to those for the X polarization except that subscripts *x* and *i* interchange positions with *y* and *j* respectively.

IV. IMPLEMENTATION AND RESULTS

The above technique has been applied in the computation of cross-talk between tracks in a PCB-on-motherboard configuration. A 1.6mm thick, 35µ Cu plated, glass-epoxy PCB, size 4.7" x 6.2", having a track pattern shown in Fig. 3, was used. L01 was the excitation point with cross-talk being measured at L31.Subsequent-ly excitation & measurement points were interchanged, giving 2 sets of measurements. The remaining 36 tracks were terminated in 50 Ω. Track thickness was 50mils and track spacing was in multiples of 50mils. Via diameter was 0.8mm with

1.6mm pads. Excitation and measurement were done using a R3763A Vector Network Analyzer in the frequency range 200Mhz to 1Ghz.

Meshing was done on a groups-of-vertical-layers basis, with each group of layers (XY plane) having the same mesh pattern. The innermost layers comprising the PCB and its immediate air regions had maximum mesh density and minimum thickness, while successive outer groups of layers were of increasing thickness and decreasing mesh density. The smallest mesh size was 12.5 x 12.5 x 12.5 mils in the inner layers and was governed by the need to model the via holes by at least 2 x 2 meshes. The outermost Z boundary layers had cubic 200mil meshes.

Multi-gridding was used extensively to reduce the total number of meshes to a manageable figure of 1.25×10^6, with one dimensional multi-gridding being used in each vertical layer & two-dimensional multi-gridding used to interface adjacent groups of layers having different mesh patterns. Multi-gridding was also used to interface the inner XY layers with wider outer XY layers so that XY boundary regions, too, had cubic 200mil meshes.

For the TLM simulation, a cosine-modulated Gausssian pulse was used as excitation, and output obtained for 100,000 time-steps, with $\Delta t = 0.5295$ ps. The output frequency response was obtained via a 1048576 point FFT with a resolution of 1.8Mhz. Run times were 200 hrs on a PIII 550Mhz PC with 128MB RAM.

The results for both simulations are shown in Fig. 4 and it is seen that they match quite well with the experimentally measured values. Surprisingly, even though L01 and L31 are not symmetrically located with respect to the PCB track pattern, both sets of simulated & measured responses (source @ L01 & @ L31) are identical.

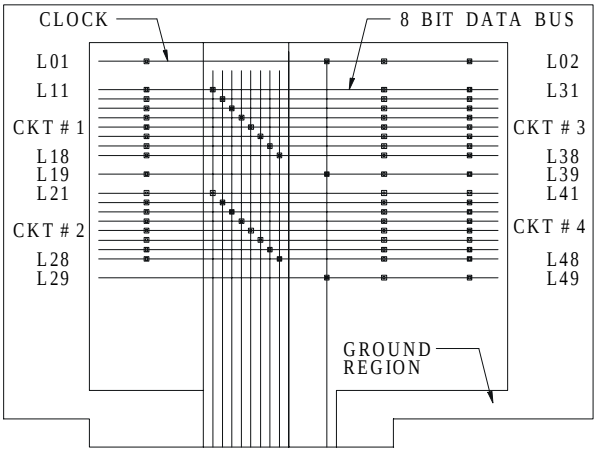

Fig. 3. Vertical PCB track pattern (double-sided)

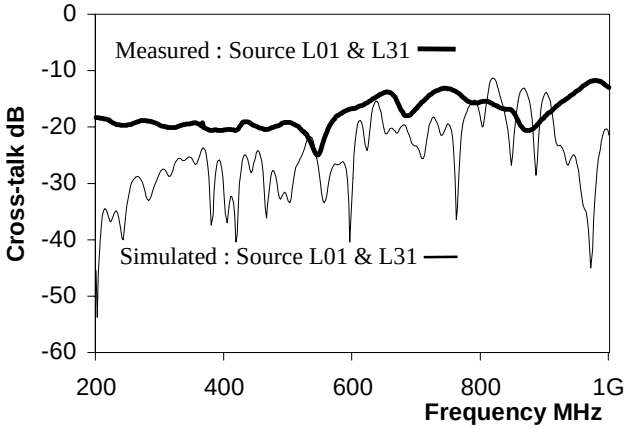

Fig. 4. Calculated and observed cross-talk between PCB tracks

In this paper, the extension of the TLM multi-gridding technique to the generalized one & two-dimensional case has been presented. The main advantage of this scheme is that separate coarse and fine mesh regions, each having meshes of the same size and shape, are not required, and a typical 'jigsaw-puzzle' meshing pattern of flush-aligned meshes of different sizes and shapes, which arises quite often in the modelling of PCB tracks, pads & vias, can be easily handled. In fact, the same mesh can simultaneously be a coarse mesh in one direction, and one of several fine meshes in another direction. This flexibility helps in greatly reducing overall mesh count as meshes in a particular area are no longer constrained to have the same size and shape.

The chief drawback of this new scheme is the additional complexity of the connection procedure and consequent increase in storage requirements and iteration time.

VI. References

[1] W. J. R. Hoefer, "The transmission-line matrix method – theory and applications," *IEEE Trans. Microwave Theory and Tech.*, vol. MTT-33, no. 10, pp. 882-893, October 1985.

[2] V. Trenkic, C. Christopoulos, and T. M. Benson, "Theory of the symmetrical super-condensed node for the TLM method," *IEEE Trans. Microwave Theory and Tech.*, vol. MTT-43, no. 6, pp. 1342-1348, June 1995.

[3] J. L. Herring and C. Christopoulos, "Multi-grid TLM method for solving EM field problems," *Electron. Lett.*, vol. 27, no. 20, pp. 1794-1795, September 1991.

[4] J. Wlodarczyk, "New multigrid interface for the TLM method," *Electron. Lett.*, vol. 32, no. 12, pp. 1111-1112, June 1996.